Feasibility of ice-penetrating radar sounding from stratospheric UAS platforms

Thomas O. Teisberg*
Stanford University
Stanford, CA, USA
teisberg@stanford.edu

Craig Mascarenhas*
Harvard University
Cambridge, MA, USA
craigmas@g.harvard.edu

Ellianna Abrahams
Stanford University
Stanford, CA, USA
ellianna@stanford.edu

Dustin M. Schroeder
Stanford University
Stanford, CA, USA
dustinms@stanford.edu

James G. Anderson
Harvard University
Cambridge, MA, USA
anderson@huarp.harvard.edu

***Abstract*—Ice-penetrating radar data, used to map the structure of Earth's ice sheets, is only available sparsely across Antarctica and Greenland due to the high cost and logistical complexity of the crewed airborne surveys currently needed to collect it. While many other remote sensing observations are now collected at high spatial and temporal resolution by satellites, the feasibility of collecting ice-penetrating radar data from Earth-orbiting satellites remains in question and no attempts have been made to date. High altitude, long endurance uncrewed aerial vehicles also promise to provide automated, long-term data collection similar to orbital platforms, while operating at speeds and altitudes that are more favorable to radar sounder link budgets and providing flexibility in flight paths. In this work, we jointly optimize a stratospheric UAS platform with an ice-penetrating radar to maximize expected signal-to-noise ratio. We analyze two candidate designs for their expected capability to map the bed beneath the Greenland and Antarctic Ice Sheets.**

***Index Terms*—HALE, UAS, ice-penetrating radar, solar aircraft, cryosphere**

I. Introduction

Ice-penetrating radar (IPR) sounders are a type of nadir-facing radar instrument used to image the englacial and subglacial structure of ice sheets and glaciers. Since the first large-scale airborne surveys in the late 1960s, a primary focus has been mapping the topography beneath the Antarctic and Greenland Ice Sheets (AIS and GIS, respectively) [1–3]. Despite decades of surveying efforts, major gaps still exist in our knowledge of the sub-glacial topography [4]. Even along Antarctica's crucial coastal margins, where local topography has a direct influence on melt rates, only about 12% of the grounding line is within 1 kilometer of an IPR survey line [5]. This data sparsity increases uncertainty in sea level rise estimates. Current topographic uncertainty around Thwaites Glacier is estimated to account for over 20 cm of uncertainty in global mean sea level rise over the next 200 years [6].

This perspective views IPR surveying as a map-building exercise, but new methods of analysis for IPR data treat the data as part of a time series. IPR data is being used to map englacial and subglacial water [7, 8], track seawater intrusion [9], estimate ice temperature [10], and infer englacial velocity [11]. Changes in these properties could be observed by repeat IPR observations.

Ice sheet surface velocity has relatively recently become available as a high spatial and temporal resolution data product enabled by surface-observing synthetic aperture radar (SAR) satellite missions [12]. The availability of this data has enabled better maps of bed topography [13], improved estimates of current ice sheet mass loss [14], and improved data-driven estimates of the fundamental physics of ice flow [15].

Ice-penetrating radar collected at similar spatial and temporal resolutions would almost certainly unlock dramatic new discoveries, however orbital platforms present significant challenges to IPR instruments. Several satellite-born IPR systems have been proposed [16–19], but concerns about achieving acceptable signal to noise ratios (SNR) [20, 21] and signal to clutter ratios (SCR) [22] have raised questions about the feasibility of these proposals. Orbital platforms are inherently very high altitude and velocity, both of which degrade the expected signal to noise ratios. Since IPR sees reflections from both surface and subsurface interfaces, the risk of off-nadir reflections overwhelming the desired reflections increases with altitude. Finally, output power and frequency selection are limited by Earth's ionosphere (effectively blocking lower frequency bands), the availability of space-qualified amplifiers (limiting output power), and spectrum allocation rules (which set limits on both frequency and power).

II. Solar-powered, stratospheric UAS as IPR platforms

The emergence of high altitude, long endurance (HALE) uncrewed aerial systems (UAS) represents a promising inter-

* T. O. Teisberg and C. Mascarenhas are co-first authors and contributed equally to this work. T. O. Teisberg was supported by a NASA FINESST Grant (80NSSC23K0271) and the TomKat Center for Sustainable Energy. We acknowledge the use of data and/or data products from CReSIS generated with support from the University of Kansas, NASA Operation IceBridge grant NNX16AH54G, NSF grants ACI-1443054, OPP-1739003, and IIS-1838230, Lilly Endowment Incorporated, and Indiana METACyt Initiative.

mediate option between the expense and complexity of low-altitude aircraft and the challenges of orbital platforms for IPR. The Stratospheric Climate Observatory System (SACOS) is a joint effort between MIT, Harvard, and Electra.aero to develop a solar-powered HALE UAS designed for climate observations [23, 24]. Flying above the tropopause, HALE systems are able to avoid most of the weather systems that complicate low-altitude polar flights. Solar powered HALE aircraft are ideally suited for operations in polar regions during summertime, with close to 24 hours of daylight providing energy for continuous surveying missions over up to about 4 months over each pole. While HALE systems fly significantly higher than other aircraft ($\sim$ 12 km versus $\sim$ 1 km over polar regions), most designs are capable of flying much slower than crewed aircraft, facilitating longer dwell times to improve IPR SNR [25]. Additionally, sub-orbital systems are friendlier to lower-TRL components, as instrument components do not need to survive a space environment and can be replaced between seasons.

While solar-powered HALE platforms only provide coverage over part of the year in polar regions, they are taskable and can spend all of the summer season over specific targets of interest. This capability means that a HALE UAS could be used to fly over critical flux gates or perform repeat monitoring timed with events such as tides. This is in contrast to orbital systems which can generally only spend a fraction of their time over polar regions and where tasking requires burning through a non-replenishable supply of fuel.

These advantages make HALE UAS appealing platforms for remedying the IPR data sparsity challenge. Using a multidisciplinary design optimization tool developed for SACOS [26], we explore the joint optimization of a HALE platform with an IPR instrument.

III. Joint optimization of aircraft and instrument

The complex and highly-coupled systems involved in the design of a solar-powered HALE aircraft necessitate a Multidisciplinary Optimization (MDO) approach for design and analysis. The Dawn Design Tool (DDT) is a dedicated MDO tool developed by the SACOS program, that sizes and designs a solar-powered aircraft by simultaneously solving the aircraft physics, energy balance, trajectory and operational considerations, and various other factors. Depending on various input factors such as the geographical location of a mission, the time of year, the required duration of the mission, and the payload properties such as weight, size, and power, the tool can investigate whether continuous flight from a solar aircraft design is feasible from a net energy perspective, and if it is, what the optimal configuration is, depending on the objective that is being designed for. The DDT involves hundreds of variables and models, and thousands of constraints. These include 2D aerodynamics, 3D aerodynamics, mass and sizing models, structures and associated solvers, atmospheric libraries, wind data, geophysical libraries, and key technology assumptions. We briefly review our use of the tool here. For details of the optimization approach, aircraft model, and examples, we refer to previous literature [23, 24, 26].

A. Simulation of aircraft system performance

Due to aero-structural failures prevalent in this class of aircraft, the default objective function for the DDT has been minimizing wingspan while achieving threshold mission success. In this study, however, an objective function was developed in order to maximize the predicted achievable surface SNR. In order to enable this, the instrument physics were coupled within the aircraft model. The basis for such an integrated approach with the DDT has been demonstrated previously [27]. This process needs to be dynamically coupled as opposed to in stages in order to capture the effect that variables such as flight altitude and ground speed have on both aircraft and instrument performance.

For a given set of mission and payload requirements, input parameters, and constraints, the output of the design tool is the convergence to a singular optimal aircraft design point based on the objective. The resulting output defines all facets of the aircraft including the aircraft size (e.g. wingspan, take-off gross weight), the configuration (e.g. number and size of propellers), the mass breakdown of various subsystems, the energy balance of various subsystems, operating specifications (e.g. cruise altitude, thrust, airspeed), and payload metrics such as utilized payload power.

Key drivers of the results include solar properties such as solar irradiation and angle based on the time of year and location. Similarly, the height of the tropopause is particularly relevant as the aircraft is constrained to operate in the stratosphere, above turbulent weather and where solar flux is predictable and unimpeded. Assumptions about key technologies such as battery energy densities, solar cell efficiency, and so on, are based on current technologies that are reasonably procurable.

B. Simulation of radar system performance

A simple model of the IPR instrument is integrated with the DDT. To assess feasibility for an IPR instrument, we focus on the expected SNR at the ice-bed interface. The power returned to a radar instrument from a reflection off of a flat, specular interface, such as the surface of an ice sheet, from the first fresnel zone may be estimated as [28, Equation S.28]:

$$P_{\text{surface}} = \frac{P_t G_t G_r \lambda^2 |\Gamma_{\text{surface}}|^2}{(4\pi h)^2} \quad (1)$$

Where P_t is the transmit power, G_t and G_r are the transmit and receive antenna gains, λ is the wavelength, $|\Gamma|^2$ is the power reflection coefficient, and h is the altitude of the radar above the surface.

While the surface reflection can be relatively well characterized, englacial reflections are most difficult to estimate due to a wide range of attenuation rates within ice and unknown reflection coefficients at the ice-bed interface, among other uncertainties. As an alternative, we follow the methodology introduced in [20] and use a data-driven estimate of the required surface SNR (RSSNR), defined as the SNR needed on the surface reflection to have a 0 dB ice-bed interface SNR after correcting for geometric spreading. To extend this approach to the GIS, we use radar sounder data collected by the University of Kansas as part of Operation IceBridge [29] and apply the same methodology as [20] to estimate RSSNR over the GIS. Following this approach, we optimize for surface SNR and use RSSNR to estimate the expected basal SNR.

Pulse length and pulse repetition interval are set by three constraints:

1) The pulse length must be less than the round trip travel time for a surface reflection
2) The pulse repetition interval must be long enough that the next pulse does not start until a pulse from a 5 kilometer sub-ice interface would have returned (”one pulse in the air”)
3) The pulse length must be short enough that the surface return and a basal return from 75% of the expected ice thickness do not overlap

This final constraint is designed to remove any issues of sidelobes from the surface overwhelming the basal echo. It is a dynamic constraint in the sense that it is calculated for each point over the ice sheet and limits the available pulse compression gain in thinner regions.

For simplicity, we assume a single transmit antenna and a single receive antenna. The total approximate mass of the IPR system is assumed to be related to the radar's peak output power by an exponential fit to the mass of selected Class AB power amplifiers. Pulse compression and coherent summation gains over one Fresnel zone are included in all SNR figures. Other parameters of the radar system are shown in Table I.

TABLE I
RADAR PARAMETERS

Frequency	60	MHz
Bandwidth	10	MHz
Antenna Gain	3	dBi
Noise Temperature	290	K
Transmit Power	1 - 1,000	W
Surface Reflectivity	-10	dB

C. Optimization process

The Dawn Design Tool optimizes for a single objective, in this case maximizing predicted surface SNR of the radar instrument. To consider a range of possible designs, we first ran the design tool independently for a range of target latitudes (spanning each ice sheet at 5 degree resolution) and for three different wingspan lengths (15 m, 25 m, and 35 m). Based on an assessment of the resulting configurations, two candidate designs (wingspan and radar power) were selected from these runs and the design tool was re-run with these parameters fixed for a range of mission lengths (1 month through 4 months).

IV. CANDIDATE DESIGNS

We present results from two candidate designs. The 15-meter wingspan design achieves very promising SNR across most of the AIS, however it is limited by the smaller amount of solar energy captured by the available solar panel area and can only support somewhat shorter missions. In addition to supporting a much higher power IPR instrument, the 25 meter design is capable of flying over nearly every part of the AIS for at least 11 weeks during the austral summer and the GIS for 10 weeks during the boreal summer. Predicted basal SNR over Antarctica is shown for each system in Figure 1. Viable mission extents are shown in Figure 2.

A. Design 1: 15 meter wingspan

At a 15 meter wingspan, the payload power and mass budgets are highly constrained. Despite these limitations, the 15 meter design achieves 40 dB estimated basal SNR across 88% of the AIS and 56% of the GIS. The 15 meter design has a relatively short viable season of about 3 weeks per year at latitudes beyond 65 degrees north or south but is capable of an 11 week season beyond 70 degrees. Selected specifications of this design are shown in Table II. The “max nominal” altitude and airspeed refers to the highest cruise altitude and airspeed across the range of latitudes considered.

TABLE II
15 METER WINGSPAN DESIGN SPECIFICATIONS

Wingspan	15	m
Gross Take-off Mass	124	kg
Max Nominal Altitude	13	km
Max Nominal Airspeed	23	m/s
Payload Mass	4	kg
Payload Power	65	W
Peak Transmit Power	60	W
Transmit Duty Cycle	35	%

B. Design 2: 25 meter wingspan

A 25 meter wingspan design allows for greater mission flexibility, with an 11 week season feasible above or below 60 degrees north or south. This is especially impactful in southern Greenland, an area where the 15 meter wingspan version has a limited season of viability. Additionally, the larger vehicle supports a heavier payload, enabling an 800 W peak transmit IPR for a roughly 10 dB better link budget.

TABLE III
25 METER WINGSPAN DESIGN SPECIFICATIONS

Wingspan	25	m
Gross Take-off Mass	290	kg
Max Nominal Altitude	13	km
Max Nominal Airspeed	22	m/s
Payload Mass	20	kg
Payload Power	650	W
Peak Transmit Power	800	W
Max Transmit Duty Cycle	35	%

V. DISCUSSION

With a potential 2-3 month season over each ice sheet, the data collection potential of a HALE UAS-borne IPR system is transformative. A single vehicle traveling at an average ground speed of 20 m/s can collect 52,560 line-km of data per

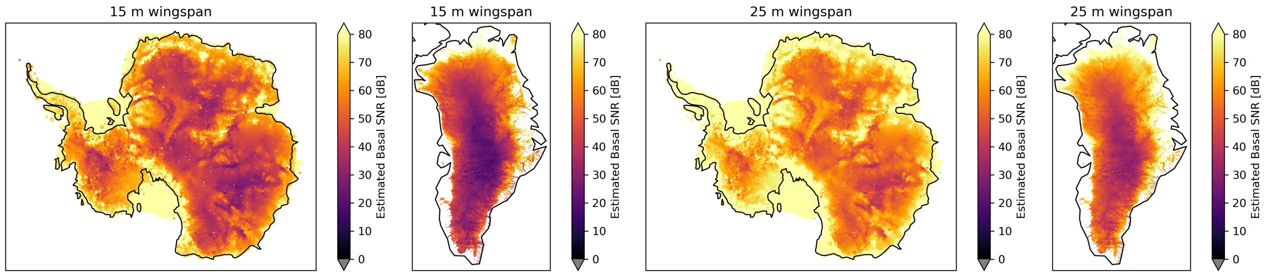

Fig. 1. Estimated SNR of basal reflection for the 15 meter wingspan design (left) and the 25 meter wingspan design (right) over the AIS based on estimated required surface SNR.

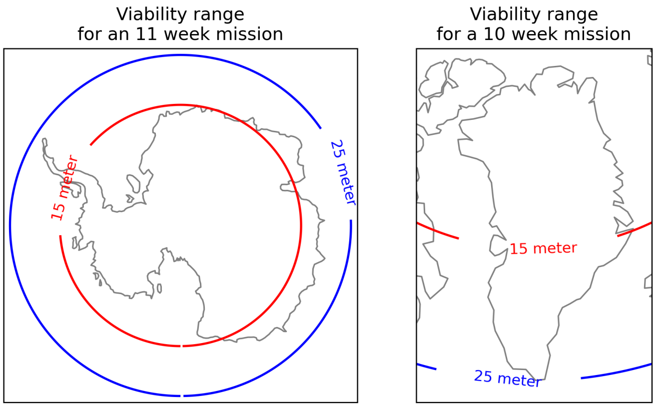

Fig. 2. The viable mission length is limited primarily by solar flux and is thus a function of latitude. Left: Northernmost latitudes continuously accessible during an 11 week AIS mission. Right: Southernmost latitudes continuously accessible during a 10 week GIS mission.

month. To put this in perspective, NASA's Operation IceBridge collected roughly 580,000 line-km of IPR data over a 10 year period [13]. This volume of data could be collected in just 3 years of 4-month missions with a HALE UAS. In Antarctica, the international community collected an average of about 85,000 line-km between 2000 and 2020, as estimated from BedMap 2 and BedMap 3 data releases [30, 31]. A single HALE UAS performing a 2 month mission to Antarctica would exceed this annual data volume.

This analysis suggests that achieving sufficient SNR for a HALE UAS-borne IPR is feasible, even for a relatively small aircraft. Thermal noise is not always the limiting factor in IPR measurements, though, and some aspects of these radar designs have not been extensively tested. One of the redeeming qualities of higher altitude systems is that they may coherently integrate over a longer distance by focusing [32]. This gain accounts for over 45 dB of SNR improvement, dramatically exceeding typical values for low-altitude aircraft [33], which will require precise relative positioning of the aircraft.

As the platform altitude increases, the antennas also become sensitive to surface and sub-surface clutter from a larger area. This clutter results from off-nadir scattering from surface or near-surface interfaces that may exist at the same reflection time as a desired englacial or subglacial interface. This is especially true for interior regions of each ice sheet, where the presence of firn creates an opportunity for numerous additional near-surface reflections, though this effect becomes less pronounced at lower frequencies, where the firn layers are smoother relative to the wavelength [22].

In this work, we focus on the detectability of the basal interface, but englacial layering is also a target of interest. Both off-nadir clutter and surface sidelobes are obstacles to detecting these shallower interfaces, especially at high altitudes. Additional work is needed to quantitatively assess the SNR required to image these interfaces.

While HALE systems are not limited in frequency selection by the ionosphere [34], licenses would still need to be granted for a high-power IPR operating at wide bandwidth.

VI. Conclusions

IPR is a very promising early payload for HALE UAS. While there are proposals, there are currently no Earth-orbiting IPR instruments, so HALE UAS compete directly with the expensive logistics of crewed aircraft in remote locations. Flying above the tropopause, HALE aircraft can also avoid many of the polar storms that complicate low-altitude logistics.

The link budgets developed in this work suggest that even a relatively small 15 meter wingspan HALE UAS could image the bed beneath most of the AIS. Due to the continuous collection capabilities, the data volume that could be collected by a single aircraft in each season would exceed the average annual IPR data collection efforts of all nations in Antarctica.

The development of a reliable HALE UAS platform remains the primary technical obstacle. As previously noted, many experiments have ended with structural failures, often as a result of weather. While the high solar fluxes make polar regions appealing for solar UAS, the weather patterns can be unpredictable, posing potential additional challenges.

On the instrument side, further validation of link budgets for higher altitude platforms is needed. This could be done with a mix of conventional crewed aircraft flying at varying altitudes and high-altitude balloons or airships.

While technical challenges remain on both the platform and sensor sides, HALE UAS-borne IPR holds the potential to change the game on IPR data collection, potentially helping to transform the sub-surface of Earth's ice sheets from a data poor to a data rich environment.

REFERENCES

[1] D. Drewry, S. Jordan, and E. Jankowski, "Measured Properties of the Antarctic Ice Sheet: Surface Configuration, Ice Thickness, Volume and Bedrock Characteristics," *Annals of Glaciology*, vol. 3, pp. 83–91, 1982. [Online]. Available: https://www.cambridge.org/core/product/identifier/S0260305500002573/type/journal_article

[2] G. D. Q. Robin, D. Drewry, and D. Meldrum, "International Studies of Ice Sheet and Bedrock," *Philosophical Transactions of the Royal Society of London. Series B, Biological Sciences*, vol. 279, no. 963, pp. 185–196, 1997. [Online]. Available: https://www.jstor.org/stable/2417761

[3] R. G. Bingham and M. J. Siegert, "Radio-Echo Sounding Over Polar Ice Masses," *Journal of Environmental and Engineering Geophysics*, vol. 12, no. 1, pp. 47–62, Mar. 2007. [Online]. Available: https://library.seg.org/doi/10.2113/JEEG12.1.47

[4] H. D. Pritchard, "Bedgap: where next for Antarctic subglacial mapping?" *Antarctic Science*, p. 16, 2014.

[5] K. Matsuoka, R. Forsberg, F. Ferraccioli, G. Moholdt, and M. Morlighem, "Circling Antarctica to Unveil the Bed Below Its Icy Edge," *Eos*, vol. 103, Jun. 2022. [Online]. Available: https://eos.org/features/circling-antarctica-to-unveil-the-bed-below-its-icy-edge

[6] B. A. Castleman, N.-J. Schlegel, L. Caron, E. Larour, and A. Khazendar, "Derivation of bedrock topography measurement requirements for the reduction of uncertainty in ice-sheet model projections of Thwaites Glacier," *The Cryosphere*, vol. 16, no. 3, pp. 761 – 778, Mar. 2022.

[7] A. K. Kendrick, D. M. Schroeder, W. Chu, T. J. Young, P. Christoffersen, J. Todd, S. H. Doyle, J. E. Box, A. Hubbard, B. Hubbard, P. V. Brennan, K. W. Nicholls, and L. B. Lok, "Surface Meltwater Impounded by Seasonal Englacial Storage in West Greenland," *Geophysical Research Letters*, vol. 45, no. 19, pp. 10,474–10,481, 10 2018.

[8] W. Chu, D. M. Schroeder, and M. R. Siegfried, "Retrieval of Englacial Firn Aquifer Thickness From Ice-Penetrating Radar Sounding in Southeastern Greenland," *Geophysical Research Letters*, vol. 45, no. 21, pp. 11,770–11,778, 11 2018.

[9] D. M. Schroeder, A. M. Hilger, J. D. Paden, D. A. Young, and H. F. J. Corr, "Ocean access beneath the southwest tributary of Pine Island Glacier, West Antarctica," *Annals of Glaciology*, vol. 59, no. 76pt1, pp. 10–15, Jul. 2018. [Online]. Available: https://www.cambridge.org/core/product/identifier/S0260305517000453/type/journal_article

[10] A. L. Broome, D. M. Schroeder, and J. T. Johnson, "Joint Active and Passive Microwave Thermometry of Ice Sheets," *IEEE Transactions on Geoscience and Remote Sensing*, vol. 61, pp. 1–10, 2023. [Online]. Available: https://ieeexplore.ieee.org/document/10065462/

[11] J. Kingslake, R. C. A. Hindmarsh, G. Aalgeirsdóttir, H. Conway, H. F. J. Corr, F. Gillet-Chaulet, C. Martín, E. C. King, R. Mulvaney, and H. D. Pritchard, "Full-depth englacial vertical ice sheet velocities measured using phase-sensitive radar: Measuring englacial ice velocities," *Journal of Geophysical Research: Earth Surface*, vol. 119, no. 12, pp. 2604–2618, Dec. 2014. [Online]. Available: http://doi.wiley.com/10.1002/2014JF003275

[12] E. Rignot, J. Mouginot, B. Scheuchl, and S. Jeong, "Changes in Antarctic Ice Sheet Motion Derived From Satellite Radar Interferometry Between 1995 and 2022," *Geophysical Research Letters*, vol. 49, no. 23, p. e2022GL100141, Dec. 2022. [Online]. Available: https://agupubs.onlinelibrary.wiley.com/doi/10.1029/2022GL100141

[13] M. Morlighem, C. N. Williams, E. Rignot, L. An, J. E. Arndt, J. L. Bamber, G. Catania, N. Chauché, J. A. Dowdeswell, B. Dorschel, I. Fenty, K. Hogan, I. Howat, A. Hubbard, M. Jakobsson, T. M. Jordan, K. K. Kjeldsen, R. Millan, L. Mayer, J. Mouginot, B. P. Y. Noël, C. O'Cofaigh, S. Palmer, S. Rysgaard, H. Seroussi, M. J. Siegert, P. Slabon, F. Straneo, M. R. van den Broeke, W. Weinrebe, M. Wood, and K. B. Zinglersen, "BedMachine v3: Complete Bed Topography and Ocean Bathymetry Mapping of Greenland From Multibeam Echo Sounding Combined With Mass Conservation," *Geophysical Research Letters*, vol. 44, no. 21, Nov. 2017. [Online]. Available: https://onlinelibrary.wiley.com/doi/10.1002/2017GL074954

[14] J. Mouginot, E. Rignot, A. A. Bjørk, M. Van Den Broeke, R. Millan, M. Morlighem, B. Noël, B. Scheuchl, and M. Wood, "Forty-six years of Greenland Ice Sheet mass balance from 1972 to 2018," *Proceedings of the National Academy of Sciences*, vol. 116, no. 19, pp. 9239–9244, May 2019. [Online]. Available: https://pnas.org/doi/full/10.1073/pnas.1904242116

[15] J. D. Millstein, B. M. Minchew, and S. S. Pegler, "Ice viscosity is more sensitive to stress than commonly assumed," *Communications Earth & Environment*, vol. 3, no. 1, p. 57, Mar. 2022. [Online]. Available: https://www.nature.com/articles/s43247-022-00385-x

[16] E. Heggy, P. A. Rosen, R. Beatty, T. Freeman, and Y. Gim, "Orbiting Arid Subsurface and Ice Sheet Sounder (OASIS):," *2013 IEEE International Geoscience and Remote Sensing Symposium - IGARSS*, pp. 3483–3486, 1 2013.

[17] P. Gogineni, C. R. Simpson, J.-B. Yan, C. R. O'Neill, R. Sood, S. Z. Gurbuz, and A. C. Gurbuz, "A CubeSat Train for Radar Sounding and Imaging of Antarctic Ice Sheet," *IGARSS 2018 - 2018 IEEE International Geoscience and Remote Sensing Symposium*, vol. 00, pp. 4138–4141, 2018.

[18] L. Carrer, C. Gerekos, F. Bovolo, and L. Bruzzone, "Distributed Radar Sounder: A Novel Concept for Subsurface Investigations Using Sensors in Formation Flight," *IEEE Transactions on Geoscience and Remote Sensing*, vol. 57, no. 12, pp. 9791–9809, 2019.

[19] M. S. Haynes, R. M. Beauchamp, A. Khazendar, R. Mazouz, M. B. Quadrelli, P. Focardi, R. E. Hodges, W. Bertiger, and N. Bienert, "Debris: Distributed Element Beamformer Radar for Ice and Subsurface Sounding," *2021 IEEE International Geoscience and Remote Sensing Symposium IGARSS*, vol. 00, pp. 651–654, 2021.

[20] D. M. Schroeder, N. L. Bienert, R. Culberg, E. J. MacKie, T. O. Teisberg, W. Chu, and D. A. Young, "Glaciological Constraints on Link Budgets for Orbital Radar Sounding of Earth's Ice Sheets," in *2021 IEEE International Geoscience and Remote Sensing Symposium IGARSS*. Brussels, Belgium: IEEE, Jul. 2021, pp. 647–650. [Online]. Available: https://ieeexplore.ieee.org/document/9553237/

[21] D. M. Schroeder and T. O. Teisberg, "Platform Altitude and Velocity Constraints on the Detectability of Subsurface Interfaces in Radar Sounding Data," in *IGARSS 2024 - 2024 IEEE International Geoscience and Remote Sensing Symposium*. Athens, Greece: IEEE, Jul. 2024, pp. 10 976–10 979. [Online]. Available: https://ieeexplore.ieee.org/document/10641853/

[22] R. Culberg and D. M. Schroeder, "Firn Clutter Constraints on the Design and Performance of Orbital Radar Ice Sounders," *IEEE Transactions on Geoscience and Remote Sensing*, vol. 58, no. 9, pp. 6344–6361, Sep. 2020. [Online]. Available: https://ieeexplore.ieee.org/document/9031695/

[23] A. Dewald, C. Mascarenhas, J. Dykema, and J. Anderson, "Feasibility and Sensitivity Analysis of Integrated Synthetic Aperture Radar (SAR) on HALE Aircraft for Wildfire Applications," in *AIAA AVIATION FORUM AND ASCEND 2024*. Las Vegas, Nevada: American Institute of Aeronautics and Astronautics, Jul. 2024. [Online]. Available: https://arc.aiaa.org/doi/10.2514/6.2024-4298

[24] C. A. Mascarenhas, J. Anderson, and J. Langford, "Solar-Powered Aircraft Feasibility Analysis based on Propulsion System Characteristics," in *AIAA AVIATION 2022 Forum*. Chicago, IL & Virtual: American Institute of Aeronautics and Astronautics, Jun. 2022. [Online]. Available: https://arc.aiaa.org/doi/10.2514/6.2022-3283

[25] T. O. Teisberg, A. L. Broome, and D. M. Schroeder, "Open Radar Code Architecture (ORCA): A Platform for Software-Defined Coherent Chirped Radar Systems," *IEEE Transactions on Geoscience and Remote Sensing*, vol. 62, pp. 1–11, 2024. [Online]. Available: https://ieeexplore.ieee.org/document/10639440/

[26] P. Sharpe, A. J. Dewald, and J. Hansman, "An Optimization Approach to Mapping the Feasible Mission Space of a High-Altitude Long-Endurance Solar Aircraft," in *AIAA AVIATION 2021 FORUM*. American Institute of Aeronautics and Astronautics, Aug. 2021. [Online]. Available: https://arc.aiaa.org/doi/10.2514/6.2021-2451

[27] A. Dewald, "An integrated vehicle, payload, and trajectory optimization framework for highly-coupled aircraft systems," Ph.D. Dissertation, Massachusetts Institute of Technology, Cambridge, MA, 2024.

[28] M. S. Haynes, "Surface and subsurface radar equations for radar sounders," *Annals of Glaciology*, vol. 61, no. 81, pp. 135–142, Apr. 2020. [Online]. Available: https://www.cambridge.org/core/product/identifier/S0260305520000166/type/journal_article

[29] CReSIS, "Radar Depth Sounder Data," 2009-2023, lawrence, Kansas, USA. [Online]. Available: http://data.cresis.ku.edu/

[30] P. Fretwell, H. D. Pritchard, D. G. Vaughan, J. L. Bamber, N. E. Barrand, R. Bell, C. Bianchi, R. G. Bingham, D. D. Blankenship, G. Casassa, G. Catania, D. Callens, H. Conway, A. J. Cook, H. F. J. Corr, D. Damaske, V. Damm, F. Ferraccioli, R. Forsberg, S. Fujita, Y. Gim, P. Gogineni, J. A. Griggs, R. C. A. Hindmarsh, P. Holmlund, J. W. Holt, R. W. Jacobel, A. Jenkins, W. Jokat, T. Jordan, E. C. King, J. Kohler, W. Krabill, M. Riger-Kusk, K. A. Langley, G. Leitchenkov, C. Leuschen, B. P. Luyendyk, K. Matsuoka, J. Mouginot, F. O. Nitsche, Y. Nogi, O. A. Nost, S. V. Popov, E. Rignot, D. M. Rippin, A. Rivera, J. Roberts, N. Ross, M. J. Siegert, A. M. Smith, D. Steinhage, M. Studinger, B. Sun, B. K. Tinto, B. C. Welch, D. Wilson, D. A. Young, C. Xiangbin, and A. Zirizzotti, "Bedmap2: improved ice bed, surface and thickness datasets for Antarctica," *The Cryosphere*, vol. 7, no. 1, pp. 375–393, Feb. 2013. [Online]. Available: https://www.the-cryosphere.net/7/375/2013/

[31] A. C. Frémand, P. Fretwell, J. A. Bodart, H. D. Pritchard, A. Aitken, J. L. Bamber, R. Bell, C. Bianchi, R. G. Bingham, D. D. Blankenship, G. Casassa, G. Catania, K. Christianson, H. Conway, H. F. J. Corr, X. Cui, D. Damaske, V. Damm, R. Drews, G. Eagles, O. Eisen, H. Eisermann, F. Ferraccioli, E. Field, R. Forsberg, S. Franke, S. Fujita, Y. Gim, V. Goel, S. P. Gogineni, J. Greenbaum, B. Hills, R. C. A. Hindmarsh, A. O. Hoffman, P. Holmlund, N. Holschuh, J. W. Holt, A. N. Horlings, A. Humbert, R. W. Jacobel, D. Jansen, A. Jenkins, W. Jokat, T. Jordan, E. King, J. Kohler, W. Krabill, M. Kusk Gillespie, K. Langley, J. Lee, G. Leitchenkov, C. Leuschen, B. Luyendyk, J. MacGregor, E. MacKie, K. Matsuoka, M. Morlighem, J. Mouginot, F. O. Nitsche, Y. Nogi, O. A. Nost, J. Paden, F. Pattyn, S. V. Popov, E. Rignot, D. M. Rippin, A. Rivera, J. Roberts, N. Ross, A. Ruppel, D. M. Schroeder, M. J. Siegert, A. M. Smith, D. Steinhage, M. Studinger, B. Sun, I. Tabacco, K. Tinto, S. Urbini, D. Vaughan, B. C. Welch, D. S. Wilson, D. A. Young, and A. Zirizzotti, "Antarctic Bedmap data: Findable, Accessible, Interoperable, and Reusable (FAIR) sharing of 60 years of ice bed, surface, and thickness data," *Earth System Science Data*, vol. 15, no. 7, pp. 2695–2710, Jul. 2023. [Online]. Available: https://essd.copernicus.org/articles/15/2695/2023/

[32] D. M. Schroeder, D. Castelletti, and I. Pena, "Revisting the Limits of Azimuth Processing Gain for Radar Sounding," in *IGARSS 2019 - 2019 IEEE International Geoscience and Remote Sensing Symposium*. Yokohama, Japan: IEEE, Jul. 2019, pp. 994–996. [Online]. Available: https://ieeexplore.ieee.org/document/8898737/

[33] M. Peters, D. Blankenship, S. Carter, S. Kempf, D. Young, and J. Holt, "Along-Track Focusing of Airborne Radar Sounding Data From West Antarctica for Improving Basal Reflection Analysis and Layer Detection," *IEEE Transactions on Geoscience and Remote Sensing*, vol. 45, no. 9, pp. 2725–2736, Sep. 2007. [Online]. Available: http://ieeexplore.ieee.org/document/4294104/

[34] A. Freeman, X. Pi, and E. Heggy, "Radar Sounding Through the Earth's Ionosphere at 45 MHz," *IEEE Transactions on Geoscience and Remote Sensing*, vol. 55, no. 10, pp. 5833–5842, Oct. 2017. [Online]. Available: http://ieeexplore.ieee.org/document/7984840/